Lattice model for the quantum anomalous Hall effect in moiré graphene

Ahmed Khalifa,[1] Ganpathy Murthy,[1] and Ribhu K. Kaul[2]

[1]*Department of Physics and Astronomy, University of Kentucky, Lexington, Kentucky 40506, USA*
[2]*Department of Physics, The Pennsylvania State University, University Park, Pennsylvania 16802, USA*

Inspired by experiments on magic angle-twisted bilayer graphene, we present a lattice mean-field model for the quantum anomalous Hall effect in a moiré setting. Our hopping Hamiltonian provides a simple route to a moiré Chern insulator in commensurately twisted systems. We study our model in the ribbon geometry and demonstrate the presence of thick chiral edge states that have a transverse localization that scales with the moiré lattice spacing. We also study the electronic structure of a domain wall between opposite Chern insulators. Our model and results are relevant to experiments that will image or manipulate the moiré quantum anomalous Hall edge states.

I. INTRODUCTION

In a remarkable burst of experimental progress, magic angle-twisted bilayer graphene has been found to host a wide range of novel quantum phenomena from band topology to superconductivity [1–7]. Notable among the states of matter discovered is the quantum anomalous Hall effect (QAHE), in which time-reversal symmetry is spontaneously broken resulting in a quantized Hall conductance [4,5,7,8]. This phenomenon, which will be the focus of this paper, brings together in a new setting the two pillars of the contemporary study of quantum materials: strong correlations and band topology, all in a structure made simply of carbon.

The iconic lattice description for the QAHE is Haldane's honeycomb model [9]. Although the Hamiltonian explicitly breaks time-reversal symmetry, it may be viewed as a useful mean-field description of the result of the spontaneous breaking of time-reversal symmetry by strong interactions. One starts with spinless electrons hopping on the honeycomb lattice, which results in a linear dispersion at half-filling and at low energies. This is graphene's celebrated realization of the Dirac equation in which the masslessness is protected by a combination of $\mathcal{C}_2\mathcal{T}$ symmetry where $\mathcal{C}_2$ denotes rotation by π around the z axis, and $\mathcal{T}$ denotes time reversal. Haldane's perturbation consists of an imaginary second-neighbor hopping chosen specifically to break $\mathcal{T}$ but preserve $\mathcal{C}_2$. Such a perturbation can be shown to guarantee a nonzero Chern number, giving rise to the QAHE. Although the k-space picture is convenient to establish bulk topology, the chiral edge states of the Chern insulator are best studied in the real-space ribbon geometry. These edge modes have a transverse localization length on the scale of spacing a of the underlying honeycomb lattice. Our goal in this paper is to construct a mean-field model for the QAHE in moiré graphene, formulated on a real-space lattice analogous to Haldane's model. Such a model would allow studies of the electronic structure, including the chiral models, of the QAHE state with inhomogeneity in real space, such as that arising from the presence of edges, internal domain walls, electrostatic potentials due to external gates,

density gradients, and disorder all of which play an important role in experiments on moiré graphene.

We first review a popular physical picture for the QAHE in moiré graphene [10–25]. The starting point is the continuum model [26,27] in which moiré reconstructions of the band structure at the K and K' valleys are treated independently. Close to the magic angle, the band structure consists of two almost flat bands in each valley that touch at the corners of the moiré Brillouin zone (BZ), a touching protected by $\mathcal{C}_2\mathcal{T}$. Upon applying sublattice masses on the two layers (via the alignment with a hexagonal boron nitride (h-BN) substrate [28–34]), $\mathcal{C}_2$ is broken, the two bands in each valley are gapped, and carry ± 1 Chern numbers [12,13]. By time reversal, the opposite valley has exactly the same band structure but with opposite Chern numbers ∓ 1. The QAHE occurs when the band structure has just enough electrons to fill up one of these four bands with electron-electron interactions spontaneously breaking time-reversal symmetry, resulting in a valley-polarized Chern insulator. In a mean-field [Hartree-Fock (HF)] picture of the continuum model, we may posit that the energy for the electrons in one valley is raised with respect to the other valley resulting in valley polarization. We note here that it is widely believed that the QAHE state in moiré graphene is spin polarized (in addition to the valley polarization just discussed). Since it also does not play a crucial role for the physics we are looking at, in our paper we will, henceforth, ignore the electron spin and focus on the orbital route to magnetism.

II. LATTICE MODEL

A straightforward calculation of the Hartree-Fock mean-field states on the moiré lattice is computationally prohibitive due to the huge size of the moiré unit cell. Rather than start with an interacting Hamiltonian and decouple it to obtain a mean-field description, our goal is to write a simple phenomenological one-body Hamiltonian that shows the QAH phase in the moiré system at 1/4 and 3/4 fillings (ignoring spin). Although such a model may not be faithful with respect
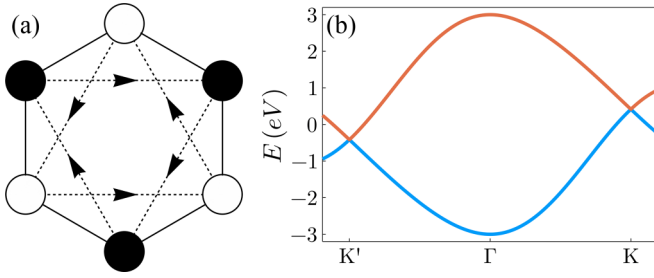
FIG. 1. The λ_{mh} perturbation of Eq. (1) on a single sheet of graphene. (a) The pattern of imaginary second-neighbor hoppings of the λ_{mh} term that breaks $\mathcal{C}_2$ and $\mathcal{T}$ individually but preserves their combination. This is a modification of the Haldane model in which the two sublattices have the imaginary hopping in the same sense; in this "modified Haldane" model they are in the opposite sense. Since λ_{mh} preserves $\mathcal{C}_2T$, it does not act as a mass term. (b) The resulting dispersion of H_{mh} in a section of the graphene Brillouin zone showing that the perturbation preserves the masslessness of the Dirac equation in each valley but raises the energy of one Dirac point with respect to the other.

to the energetics, it is adiabatically connected to the QAH state obtained from the standard HF approach and is expected to capture many of the broad features of the QAH phase especially the topological features, such as edge states. It is not obvious *a priori* how to write a mean-field lattice model that leads to the QAHE with the same mechanism as in the continuum mean-field picture. Nonetheless, inspired by the continuum picture, we seek a perturbation to the monolayer graphene Hamiltonian that raises the energy in one valley with respect to the other but maintains the masslessness of the Dirac points in each valley. The perturbation must break both $\mathcal{T}$ and $\mathcal{C}_2$ so that the band structures in the two valleys can be different but must preserve $\mathcal{C}_2\mathcal{T}$ so that the Dirac equation is left massless. Such a term can be constructed by modifying the honeycomb Haldane model, arranging for the sense of the imaginary hopping on the A and B sublattices to run oppositely (in the Haldane model, they run in the same direction). This is shown pictorially in Fig. 1,

$$H_{\mathrm{mh}} = -t \sum_{\langle i,j \rangle} c_i^\dagger c_j + \lambda_{mh} \sum_{\langle\langle i,j \rangle\rangle} i\nu_{ij} c_i^\dagger c_j, \quad (1)$$

where c_i denotes the electron's annihilation operator at honeycomb site i and $\nu_{ij} = \pm 1$. The A-a hopping and B-B hopping change sign under both $\mathcal{C}_2$ and $\mathcal{T}$ but are left invariant under the $\mathcal{C}_2\mathcal{T}$. The band structure of monolayer graphene perturbed with λ_{mh}, shown in the right panel of Fig. 1, displays the expected behavior, two massless Dirac cones at K and K' but with touching points that are displaced in energy. This model has been introduced previously and was dubbed the modified Haldane model in the context of studying antichiral edge states in two-dimensional fermion systems [35,36]. Althoughthe λ_{mh} term does not lead to a Chern insulator in monolayer graphene, we now show that when added to twisted moiré graphene, it results in the QAHE.

We now incorporate this perturbation into a lattice model of twisted bilayer graphene. In order to work on a moiré system on the lattice, we use commensurate twist angles with large moiré triangular lattice vectors $\mathbf{A}_1$ and $\mathbf{A}_2$ ($A_M \equiv |\mathbf{A}_1| = |\mathbf{A}_2|$)
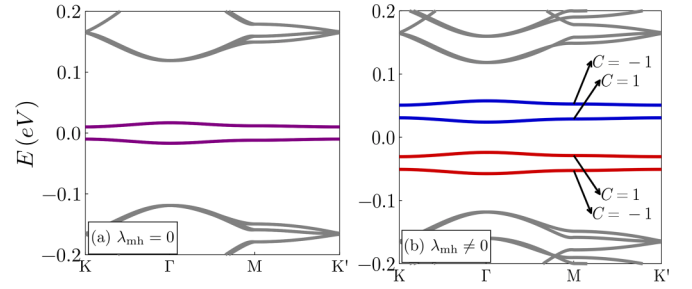

FIG. 2. The band structure of the commensurately twisted lattice model H_{TBG}, Eq. (2) in the moiré BZ computed with periodic boundary conditions (without edges). (a) Without the perturbation term, $\lambda_{\mathrm{mh}} = 0$, $\mathcal{T}$ is preserved, and a Chern insulator is not possible. The two isolated flat bands in the middle are doubly degenerate, which can be understood from the continuum model as arising due to the valley degeneracy. The remote bands in gray do not play an important role in our paper. (b) Turning on λ_{mh} breaks $\mathcal{T}$ and allows the moiré system to have bands that have well-defined Chern numbers, the arrows point to the value of the Chern number of the bands. Chern numbers are computed by the standard lattice method [47]. This spinless moiré system would be a Chern insulator at 1/4 and 3/4 fillings of the flat-band system. We used $\theta \approx 1.08°$, $t = 2.7$ eV, $t_v = 0.686$ eV, $\kappa = 0.0$, $\eta = 0.3a$, $m_t = m_b = 10$, and $\lambda_{\mathrm{mh}} = 8$ meV.

and a smaller moiré Brillouin zone [26,37,38]. To demonstrate that λ_{mh} indeed results in the QAHE in the moiré graphene, we construct a tight-binding model on the commensurate lattice [39–42] for the twisted bilayer graphene (TBG) system,

$$H_{\mathrm{TBG}} = \sum_\mu H_{\mu,\mathrm{mh}} + \sum_{\mu,i} m_\mu \sigma_z c_{\mu,i}^\dagger c_{\mu,i} + \sum_{i,j} t_{ij}^\perp c_{t,i}^\dagger c_{b,j}, \quad (2)$$

where $c_{\mu,i}$ is the annihilation operator for an electron in layer $\mu = t, b$ and at lattice position i. The first "intralayer" term, defined in Eq. (1), consists of the usual graphene hopping as well as the λ_{mh} perturbation term. The second term corresponds to the effect of the h-BN substrate, which is a staggered mass on each layer with σ_z denoting the sublattice degree of freedom. The last term corresponds to the interlayer hopping. We take a simple interlayer hopping model that is a function of the in-plane distance between two atoms in different layers and falls off exponentially with increasing distance. This gives the following form for the interlayer hopping, $t^\perp(r) = t_v \exp(-r/\eta)$, where r is the in-plane distance between the two atoms, η controls the range of the hopping and t_v is the hopping amplitude. Lattice relaxations reduce the A-A hopping between the layers in contrast to A-B hopping [43–46], which we include in the model by the parameter κ, which defines the ratio between the two.

In Fig. 2, we show the band structure of the model first with $\lambda_{\mathrm{mh}} = 0$ and then with $\lambda_{\mathrm{mh}} \neq 0$. For $\lambda_{\mathrm{mh}} = 0$, there are two flat bands that are each doubly degenerate. The degeneracy can be understand in the continuum model as arising from the two valleys. Since $\mathcal{T}$ is preserved, no Chern insulator is possible. For $\lambda_{\mathrm{mh}} \neq 0$, we observe that the flat bands split into four isolated bands (one pair moves up, and the other pair moves down in energy). As we would expect from the continuum model picture since the λ_{mh} perturbation raises the energy of one valley's Dirac touching with respect to the

other in monolayer graphene, the two flat bands in one valley move up, whereas, those in the other move down. The Chern numbers of the pair that move up are ± 1, whereas, those of the pair that move down have ∓ 1, consistent with the fact that they arose from two valleys connected by time-reversal symmetry when $\lambda_{\mathrm{mh}} = 0$. Evidently, if we fill the flat-band manifold with only enough electrons to fill one band (or three bands), we obtain a Chern insulator. This demonstrates that the λ_{mh} perturbation can turn the moiré system into a quantum anomalous Hall insulator. We note here for completeness that for a single sheet of graphene, H_{mh} supplemented with a sublattice mass term breaks $\mathcal{T}$ but, nonetheless, gives rise only to a trivial insulator; the Chern insulator that we find here for the twisted case essentially requires the subtle moiré band reconstructions.

III. EDGE STATES

Having established that the λ_{mh} perturbation creates a QAH state from the bulk k-space topology, we now study the model in a ribbon geometry to access the edge states. We construct a ribbon by taking the system to be infinite along the "longitudinal" $\mathbf{A}_2$ direction (with the momentum parallel to $\mathbf{A}_2$ being a good quantum number) and finite along the "transverse" $\mathbf{A}_1$ direction, which defines the width of the ribbon. Due to the large number of atoms in the unit cell (up to 10^5 in our paper), we use the Lanczos algorithm to obtain the bands near charge neutrality where the Chern bands and, hence, the edge states reside. Figure 3(a) shows the band structure of the Hamiltonian in Eq. (2) of a ribbon with a width of 20 moiré unit cells. We see the projection of the four bulk bands near charge neutrality, but most importantly, we see two pairs of gap crossing modes that are localized on the upper and lower edges of the ribbon that correspond to the edge states of the Chern insulator. The location of the support of the wave functions in the transverse direction is determined by computing the position expectation value of the wave function along the width of the ribbon [48]. Note that there are also edge states that lie at energies above and below the four flat bands, which are reminiscent of the "moiré edge states" that exist before adding the H_{mh} perturbation [42,48–53]. These states are counterpropagating along each edge, which makes them susceptible to backscattering in contrast with the robust edge states of the Chern insulator discussed here. Furthermore, they do not cross the band gap between the flat bands and the remote bands.

What is the transverse localization length of the edge states? Given the microscopic form of the mean-field perturbation in Eq. (1) [illustrated in Fig. 1(a)], one may naively assume that the edge states are localized on the scale of a graphene lattice spacing. On the other hand, in the continuum model, the moiré lattice spacing A_M is the only length scale that appears, and, hence, we might expect that the edge state wave function to be localized on this larger scale. We plot the edge state wave function squared amplitude in Fig. 3(b). We see that the edge mode wave functions extend up to approximately one moiré unit-cell length A_M, in agreement with the expectation from the continuum model. The fundamental graphene lattice constant a is about 50 times smaller than A_M. Furthermore, we have checked that the edge state localization
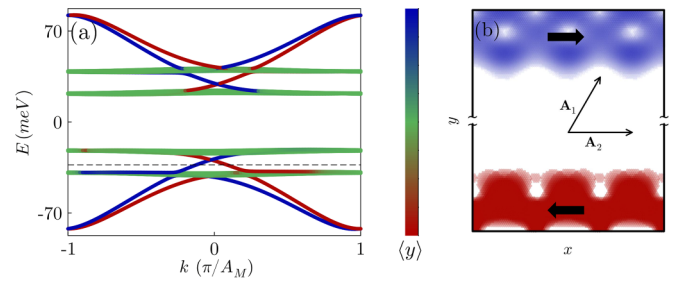

FIG. 3. Band structure and wave functions of H_{TBG} in a ribbon geometry (with edges) with the same parameters as in Fig. 2 and with a transverse width of 20 moiré unit cells and infinite longitudinal direction. (a) Shows the bands in a window of energy that includes the four flat bands of Fig. 2(b). The color of the eigenstates represents the expectation value of the transverse coordinate of the ribbon in accordance with the shown color bar. The bulk bands appear green since their average transverse coordinate is in the middle. Likewise, edge states localized on the upper (lower) edge appear blue (red). We observe that chiral midgap states show up between the first and the second and between the third and the fourth flat bands, corresponding to the edge states of a Chern insulator at 1/4 and 3/4 fillings. In addition, counterpropagating edge states not associated with the QAHE appear below the first band and above the fourth band. A possible Fermi level for a Chern insulator at bulk filling of 1/4 is shown as a dashed line. (b) Shows the details of $|\Psi|^2$ for the two edge states' wave functions at the Fermi level marked in (a). The system diagonalized had a transverse width of 20 moiré unit cells but for clarity most of the bulk has been omitted as represented by the broken y axis. For visual clarity, we have shown three repeats of the unit cell along the longitudinal direction. Black arrows indicate the chirality of the edge modes inferred from their group velocities in (a).

length depends linearly on A_M demonstrating that it is tied to this larger length scale (see the Supplemental Material [54]).

IV. DOMAIN WALLS

The QAHE phase in moiré graphene has been argued to be an orbital ferromagnet, which breaks time-reversal symmetry spontaneously [10–25]. This discrete symmetry breaking results in two ground states corresponding to clockwise or anticlockwise chiral edge states ($C = \pm 1$) connected by time-reversal symmetry, which can be accessed in our model by choosing the mean-field term λ_{mh} either positive or negative. Experiments on twisted bilayer graphene aligned with h-BN have reported the coexistence of ferromagnetic domains in the system [4,5,7,8,55] with a possible mesoscale pattern of opposite domains separated by domain walls. The domain walls themselves are fascinating objects that provide an experimentally tunable realization of the zero modes trapped by defects in topological band systems, a fundamental problem in physics [56,57]. Our model allows us to explicitly compute the wave functions of the chiral modes localized at the domain walls. To set up a domain wall, we study a configuration where the order parameter λ_{mh} varies smoothly across the width of the ribbon between two regions of opposite Chern number. We use $\lambda_{\mathrm{mh}} = \lambda_{\mathrm{mh}_0} \tanh(y/\xi)$ with ξ a characteristic length scale of the domain wall. In Fig. 4(a), we show the resulting band structure. Focusing at a Fermi level corresponding to 1/4
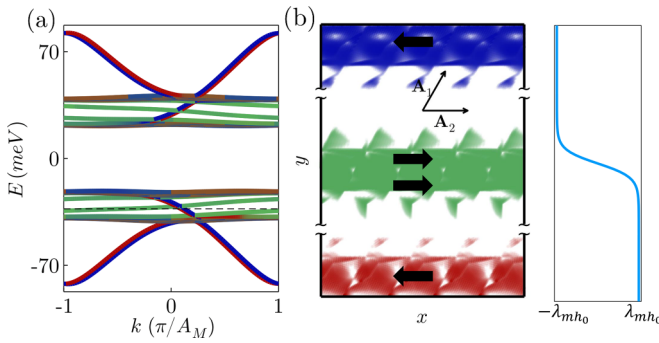
FIG. 4. Electronic structure of a QAHE domain wall in the ribbon geometry. (a) Shows the band structure in the presence of a $C = \pm 1$ domain wall (see the text), colored with the same color bar as in Fig. 3. At the Fermi level (dashed line) for 1/4 bulk filling, there are now four chiral edge states: two of these are quasidegenerate and localized in the middle (and, hence, appear green) at the domain wall, and the other two are at the upper and lower edge of the ribbon. (b) Density for the localized mode wave functions at the 1/4 Fermi level, showing the chiralities inferred from the group velocities of the band structure. For clarity, we show only one of the two modes trapped on the domain wall since they have similar support. We have shown five repeats along the longitudinal direction. The profile of the domain wall used ($\xi = 0.9A_M$) is shown on the right. All other parameters are same as in Fig. 2.

filling (shown as a dashed line), we find four localized states: two states at the center of the sample (trapped by the domain wall), and one each on the upper and lower edges. The two parallel chiral states in the domain wall are consistent with the behavior of a domain wall separating regions with $C = \pm 1$ Chern numbers. The corresponding wave function for one of the domain-wall states is shown in Fig. 4(b) exhibiting a state that is localized in the middle of the ribbon with a localization length controlled by A_M, the moiré length scale. Also shown in this figure is the upper and lower chiral edge states.

V. ENERGETICS

We have demonstrated that the λ_{mh} perturbation of Eq. (1) does indeed create a mean-field QAH state in moiré graphene, and the chiral edge modes appropriate for both a hard edge and a domain wall. Our mean-field ansatz is also conceptually attractive because it has only two "moving parts:" The sublattice masses to gap the flat bands and give them nontrivial Chern numbers in each valley, and λ_{mh} to raise one valley with respect to the other, which we have made simply arguments has to result in a Chern insulator. However, it is interesting to step back and ask whether this mean-field ansatz is unique or favored in some sense. From a symmetry point of view, the only necessary (but not sufficient) requirement to get a Chern insulator is the perturbation break $\mathcal{T}$. Clearly many imaginary hopping patterns, such as Haldane's perturbation, or those involving further neighbor hopping and modulation of the hopping with the moiré periodicity, can achieve this. However, unlike our simple ansatz, it is *a priori* unclear which of these will result in a Chern insulator. A full Hartree-Fock calculation on the lattice, including all the bands, will by definition lead to the best mean-field Hamiltonian. However, this is

computationally prohibitive. To gain further physics insight into the issue in a limited parameter space, we have constructed a mean-field model, which has the sublattice masses, the modified Haldane term with a coefficient λ_{mh}, and a Haldane term with coefficient λ_h. Note that the Haldane term by itself also leads to a Chern insulator for TBG at quarter filling. We variationally compute the total energy, including the Coulomb interaction screened by gates [10–18] as a function of λ_{mh}, λ_h for a fixed set of sublattice masses. As shown in the SM [54], we find that the minimum occurs when $\lambda_h = 0, \lambda_{mh} \neq 0$. Thus, at least, in this limited set of variational parameters, the modified Haldane term is preferred.

VI. CONCLUSION

To summarize, we have introduced a lattice mean-field model for the quantum anomalous Hall effect in twisted bilayer graphene. The mechanism that gives rise to the Chern insulator is physically appealing: The sublattice masses on the two layers break $\mathcal{C}_2$, gap out the flat bands in each valley, and give them nontrivial Chern numbers, whereas the modified Haldane term breaks $\mathcal{T}$ and raises the states in one valley with respect to the other. Our mean-field model's conceptual simplicity, its computational tractability, and its good energetics (albeit in a limited parameter space) make it attractive for study. By solving our lattice model in a ribbon geometry, we find that the chiral edge modes of the QAH state have a transverse localization length that scales with the moiré lattice spacing. We have also used our model to study the domain walls occurring between regions where the order parameter changes sign.

A number of interesting open questions involving spatially inhomogeneous systems can be studied using our lattice approach. The control of the electronic structure of the chiral modes by the shape of the domain wall, a study of networks of domain walls, and the effect of impurities are some examples. We hope to study these and other questions in the near future.

Note added. Recently, while our paper was being finalized for submission, an experimental work using scanning tunnel microscopes on domain walls in twisted monolayer-bilayer graphene has appeared in which the QAHE edge states have been imaged for the first time [58]. Although closely related to the system under study here, it is different in detail. The main idea of our theory can be adapted straightforwardly to this paper.

[1] Y. Cao, V. Fatemi, S. Fang, K. Watanabe, T. Taniguchi, E. Kaxiras, and P. Jarillo-Herrero, Unconventional superconductivity in magic-angle graphene superlattices, Nature (London) **556**, 43 (2018).

[2] Y. Cao, V. Fatemi, A. Demir, S. Fang, S. L. Tomarken, J. Y. Luo, J. D. Sanchez-Yamagishi, K. Watanabe, T. Taniguchi, E. Kaxiras, R. C. Ashoori, and P. Jarillo-Herrero, Correlated insulator behaviour at half-filling in magic-angle graphene superlattices, Nature (London) **556**, 80 (2018).

[3] M. Yankowitz, S. Chen, H. Polshyn, Y. Zhang, K. Watanabe, T. Taniguchi, D. Graf, A. F. Young, and C. R. Dean, Tuning superconductivity in twisted bilayer graphene, Science **363**, 1059 (2019).

[4] A. L. Sharpe, E. J. Fox, A. W. Barnard, J. Finney, K. Watanabe, T. Taniguchi, M. A. Kastner, and D. Goldhaber-Gordon, Emergent ferromagnetism near three-quarters filling in twisted bilayer graphene, Science **365**, 605 (2019).

[5] M. Serlin, C. L. Tschirhart, H. Polshyn, Y. Zhang, J. Zhu, K. Watanabe, T. Taniguchi, L. Balents, and A. F. Young, Intrinsic quantized anomalous Hall effect in a moiré heterostructure, Science **367**, 900 (2020).

[6] X. Lu, P. Stepanov, W. Yang, M. Xie, M. A. Aamir, I. Das, C. Urgell, K. Watanabe, T. Taniguchi, G. Zhang, A. Bachtold, A. H. MacDonald, and D. K. Efetov, Superconductors, orbital magnets and correlated states in magic-angle bilayer graphene, Nature (London) **574**, 653 (2019).

[7] G. Chen, A. L. Sharpe, E. J. Fox, Y.-H. Zhang, S. Wang, L. Jiang, B. Lyu, H. Li, K. Watanabe, T. Taniguchi, Z. Shi, T. Senthil, D. Goldhaber-Gordon, Y. Zhang, and F. Wang, Tunable correlated Chern insulator and ferromagnetism in a moiré superlattice, Nature (London) **579**, 56 (2020).

[8] S. Grover, M. Bocarsly, A. Uri, P. Stepanov, G. Di Battista, I. Roy, J. Xiao, A. Y. Meltzer, Y. Myasoedov, K. Pareek, K. Watanabe, T. Taniguchi, B. Yan, A. Stern, E. Berg, D. K. Efetov, and E. Zeldov, Chern mosaic and Berry-curvature magnetism in magic-angle graphene, Nat. Phys. **18**, 885 (2022).

[9] F. D. M. Haldane, Model for a Quantum Hall Effect without Landau Levels: Condensed-Matter Realization of the "Parity Anomaly," Phys. Rev. Lett. **61**, 2015 (1988).

[10] E. Y. Andrei and A. H. MacDonald, Graphene bilayers with a twist, Nature Mater. **19**, 1265 (2020).

[11] J. Liu and X. Dai, Orbital magnetic states in moiré graphene systems, Nat. Rev. Phys. **3**, 367 (2021).

[12] Y.-H. Zhang, D. Mao, Y. Cao, P. Jarillo-Herrero, and T. Senthil, Nearly flat Chern bands in moiré superlattices, Phys. Rev. B **99**, 075127 (2019).

[13] N. Bultinck, S. Chatterjee, and M. P. Zaletel, Mechanism for Anomalous Hall Ferromagnetism in Twisted Bilayer Graphene, Phys. Rev. Lett. **124**, 166601 (2020).

[14] F. Wu and S. Das Sarma, Collective Excitations of Quantum Anomalous Hall Ferromagnets in Twisted Bilayer Graphene, Phys. Rev. Lett. **124**, 046403 (2020).

[15] C. Repellin, Z. Dong, Y.-H. Zhang, and T. Senthil, Ferromagnetism in Narrow Bands of Moiré Superlattices, Phys. Rev. Lett. **124**, 187601 (2020).

[16] J. Shi, J. Zhu, and A. H. MacDonald, Moiré commensurability and the quantum anomalous Hall effect in twisted bilayer graphene on hexagonal boron nitride, Phys. Rev. B **103**, 075122 (2021).

[17] Y. H. Kwan, G. Wagner, N. Chakraborty, S. H. Simon, and S. A. Parameswaran, Domain wall competition in the Chern insulating regime of twisted bilayer graphene, Phys. Rev. B **104**, 115404 (2021).

[18] Y. Su and S.-Z. Lin, Current-Induced Reversal of Anomalous Hall Conductance in Twisted Bilayer Graphene, Phys. Rev. Lett. **125**, 226401 (2020).

[19] J. Liu and X. Dai, Theories for the correlated insulating states and quantum anomalous Hall effect phenomena in twisted bilayer graphene, Phys. Rev. B **103**, 035427 (2021).

[20] Y.-H. Zhang, D. Mao, and T. Senthil, Twisted bilayer graphene aligned with hexagonal boron nitride: Anomalous Hall effect and a lattice model, Phys. Rev. Res. **1**, 033126 (2019).

[21] S. Liu, E. Khalaf, J. Y. Lee, and A. Vishwanath, Nematic topological semimetal and insulator in magic-angle bilayer graphene at charge neutrality, Phys. Rev. Res. **3**, 013033 (2021).

[22] Y. Zhang, K. Jiang, Z. Wang, and F. Zhang, Correlated insulating phases of twisted bilayer graphene at commensurate filling fractions: A Hartree-Fock study, Phys. Rev. B **102**, 035136 (2020).

[23] Y.-P. Lin and R. M. Nandkishore, Chiral twist on the high-T_c phase diagram in moiré heterostructures, Phys. Rev. B **100**, 085136 (2019).

[24] T. Cea and F. Guinea, Band structure and insulating states driven by Coulomb interaction in twisted bilayer graphene, Phys. Rev. B **102**, 045107 (2020).

[25] X. Lin and J. Ni, Symmetry breaking in the double moiré superlattices of relaxed twisted bilayer graphene on hexagonal boron nitride, Phys. Rev. B **102**, 035441 (2020).

[26] J. M. B. L. dos Santos, N. M. R. Peres, and A. H. Castro Neto, Graphene Bilayer with a Twist: Electronic Structure, Phys. Rev. Lett. **99**, 256802 (2007).

[27] R. Bistritzer and A. H. MacDonald, Moiré bands in twisted double-layer graphene, Proc. Natl. Acad. Sci. USA **108**, 12233 (2011).

[28] J. Jung, A. M. DaSilva, A. H. MacDonald, and S. Adam, Origin of band gaps in graphene on hexagonal boron nitride, Nat. Commun. **6**, 6308 (2015).

[29] J. Jung, E. Laksono, A. M. DaSilva, A. H. MacDonald, M. Mucha-Kruczyński, and S. Adam, Moiré band model and band gaps of graphene on hexagonal boron nitride, Phys. Rev. B **96**, 085442 (2017).

[30] B. Hunt, J. D. Sanchez-Yamagishi, A. F. Young, M. Yankowitz, B. J. LeRoy, K. Watanabe, T. Taniguchi, P. Moon, M. Koshino, P. Jarillo-Herrero, and R. C. Ashoori, Massive Dirac fermions and Hofstadter butterfly in a van der Waals heterostructure, Science **340**, 1427 (2013).

[31] F. Amet, J. R. Williams, K. Watanabe, T. Taniguchi, and D. Goldhaber-Gordon, Insulating Behavior at the Neutrality Point in Single-Layer Graphene, Phys. Rev. Lett. **110**, 216601 (2013).

[32] A. A. Zibrov, E. M. Spanton, H. Zhou, C. Kometter, T. Taniguchi, K. Watanabe, and A. F. Young, Even-denominator fractional quantum Hall states at an isospin transition in monolayer graphene, Nat. Phys. **14**, 930 (2018).

[33] H. Kim, N. Leconte, B. L. Chittari, K. Watanabe, T. Taniguchi, A. H. MacDonald, J. Jung, and S. Jung, Accurate gap determination in monolayer and bilayer graphene/h-BN moiré superlattices, Nano Lett. **18**, 7732 (2018).

[34] D. Wong, Y. Wang, J. Jung, S. Pezzini, A. M. DaSilva, H.-Z. Tsai, H. S. Jung, R. Khajeh, Y. Kim, J. Lee, S. Kahn,

S. Tollabimazraehno, H. Rasool, K. Watanabe, T. Taniguchi, A. Zettl, S. Adam, A. H. MacDonald, and M. F. Crommie, Local spectroscopy of moiré-induced electronic structure in gate-tunable twisted bilayer graphene, Phys. Rev. B **92**, 155409 (2015).

[35] E. Colomés and M. Franz, Antichiral Edge States in a Modified Haldane Nanoribbon, Phys. Rev. Lett. **120**, 086603 (2018).

[36] L. Zhu, V. Aji, and C. M. Varma, Ordered loop current states in bilayer graphene, Phys. Rev. B **87**, 035427 (2013).

[37] E. J. Mele, Commensuration and interlayer coherence in twisted bilayer graphene, Phys. Rev. B **81**, 161405(R) (2010).

[38] S. Shallcross, S. Sharma, E. Kandelaki, and O. A. Pankratov, Electronic structure of turbostratic graphene, Phys. Rev. B **81**, 165105 (2010).

[39] G. Trambly de Laissardière, D. Mayou, and L. Magaud, Localization of Dirac electrons in rotated graphene bilayers, Nano Lett. **10**, 804 (2010).

[40] J. C. Slater and G. F. Koster, Simplified LCAO method for the periodic potential problem, Phys. Rev. **94**, 1498 (1954).

[41] P. Moon and M. Koshino, Optical absorption in twisted bilayer graphene, Phys. Rev. B **87**, 205404 (2013).

[42] W. Landgraf, S. Shallcross, K. Türschmann, D. Weckbecker, and O. Pankratov, Electronic structure of twisted graphene flakes, Phys. Rev. B **87**, 075433 (2013).

[43] N. N. T. Nam and M. Koshino, Lattice relaxation and energy band modulation in twisted bilayer graphene, Phys. Rev. B **96**, 075311 (2017).

[44] P. Lucignano, D. Alfè, V. Cataudella, D. Ninno, and G. Cantele, Crucial role of atomic corrugation on the flat bands and energy gaps of twisted bilayer graphene at the magic angle $\theta \sim 1.08°$, Phys. Rev. B **99**, 195419 (2019).

[45] S. Carr, S. Fang, Z. Zhu, and E. Kaxiras, Exact continuum model for low-energy electronic states of twisted bilayer graphene, Phys. Rev. Res. **1**, 013001 (2019).

[46] G. Cantele, D. Alfe, F. Conte, V. Cataudella, D. Ninno, and P. Lucignano, Structural relaxation and low-energy properties of twisted bilayer graphene, Phys. Rev. Res. **2**, 043127 (2020).

[47] T. Fukui, Y. Hatsugai, and H. Suzuki, Chern numbers in discretized brillouin zone: Efficient method of computing (spin) Hall conductances, J. Phys. Soc. Jpn. **74**, 1674 (2005).

[48] M. Fujimoto and M. Koshino, Moiré edge states in twisted bilayer graphene and their topological relation to quantum pumping, Phys. Rev. B **103**, 155410 (2021).

[49] E. Suárez Morell, R. Vergara, M. Pacheco, L. Brey, and L. Chico, Electronic properties of twisted bilayer nanoribbons, Phys. Rev. B **89**, 205405 (2014).

[50] E. S. Morell, P. Vargas, P. Häberle, S. A. Hevia, and L. Chico, Edge states of moiré structures in graphite, Phys. Rev. B **91**, 035441 (2015).

[51] J. Liu, J. Liu, and X. Dai, Pseudo Landau level representation of twisted bilayer graphene: Band topology and implications on the correlated insulating phase, Phys. Rev. B **99**, 155415 (2019).

[52] M. Fleischmann, R. Gupta, D. Weckbecker, W. Landgraf, O. Pankratov, V. Meded, and S. Shallcross, Moiré edge states in twisted graphene nanoribbons, Phys. Rev. B **97**, 205128 (2018).

[53] C. Ma, Q. Wang, S. Mills, X. Chen, B. Deng, S. Yuan, C. Li, K. Watanabe, T. Taniguchi, X. Du, F. Zhang, and F. Xia, Moiré band topology in twisted bilayer graphene, Nano Lett. **20**, 6076 (2020).

[54] See Supplemental Material at http://link.aps.org/supplemental/10.1103/PhysRevB.107.235137 for a review of twisted bilayer graphene with a commensurate twist angle; showing the localization of the edge states dependence on the twist angle or the moiré length scale; calculating the energy of the mean-field state in the presence of electron-electron interactions. It also contains Refs. [37,38].

[55] C. L. Tschirhart, M. Serlin, H. Polshyn, A. Shragai, Z. Xia, J. Zhu, Y. Zhang, K. Watanabe, T. Taniguchi, M. E. Huber, and A. F. Young, Imaging orbital ferromagnetism in a moiré Chern insulator, Science **372**, 1323 (2021).

[56] R. Jackiw and C. Rebbi, Solitons with Fermion number $\frac{1}{2}$, Phys. Rev. D **13**, 3398 (1976).

[57] A. J. Heeger, S. Kivelson, J. R. Schrieffer, and W. P. Su, Solitons in conducting polymers, Rev. Mod. Phys. **60**, 781 (1988).

[58] C. Zhang, T. Zhu, S. Kahn, T. Soejima, K. Watanabe, T. Taniguchi, A. Zettl, F. Wang, M. P. Zaletel, and M. F. Crommie, Visualizing and manipulating chiral edge states in a moiré quantum anomalous Hall insulator, arXiv:2212.03380.